

# CHARACTERIZATION OF CATHODE KEEPER WEAR BY SURFACE LAYER ACTIVATION

Robert D. Kolasinski  
California Institute of Technology  
Pasadena, CA

James E. Polk  
Jet Propulsion Laboratory  
California Institute of Technology  
Pasadena, CA

In this study, the erosion rates of the discharge cathode keeper in a 30 cm NSTAR configuration ion thruster were measured using a technique known as Surface Layer Activation (SLA). This diagnostic technique involves producing a radioactive tracer in a given surface by bombardment with high energy ions. The decrease in activity of the tracer material may be monitored as the surface is subjected to wear processes and correlated to a depth calibration curve, yielding the eroded depth. Analysis of the activities was achieved through a gamma spectroscopy system. The primary objectives of this investigation were to reproduce erosion data observed in previous wear studies in order to validate the technique, and to determine the effect of different engine operating parameters on erosion rate. The erosion profile at the TH 15 (2.3 kW) setting observed during the 8200 hour Life Demonstration Test (LDT) was reproduced. The maximum keeper erosion rate at this setting was determined to be 0.085  $\mu\text{m/hr}$ . Testing at the TH 8 (1.4 kW) setting demonstrated lower erosion rates than TH 15, along with a different wear profile. Varying the keeper voltage was shown to have a significant effect on the erosion, with a positive bias with respect to cathode potential decreasing the erosion rate significantly. Accurate measurements were achieved after operating times of only 40 to 70 hours, a significant improvement over other erosion diagnostic methods.

## NOMENCLATURE

$a$	Reference count rate, cps
$E_o$	Ion energy, pre-sheath
$E_w$	Ion energy, wall
$m$	Spectrum scaling parameter
$\dot{m}$	Mass flow rate, sccm
$\eta_{TOT}$	Total thruster efficiency
$P_{TOT}$	Total thruster power, W
$q$	Ion charge
$T$	Thrust, mN
$\tau$	Spectrum live time, sec
$W$	Weight factor array
$y$	Sample count rate, cps
$z$	Total counts

## Subscripts

$A$	Accelerator Grid
$B$	Beam
$b$	Background spectrum
$CK$	Cathode Keeper
$D$	Discharge
$i$	Channel
$j$	Isotope
$NK$	Neutralizer Keeper
$r$	Reference spectrum
$s$	Sample spectrum

## INTRODUCTION

Evaluating the lifetime of discharge cathodes has been of great interest throughout the history of ion engine design, since their failure modes are generally considered to be among the major life limiting mechanisms of these thrusters.<sup>1</sup> Wear processes specifically associated with the discharge cathode assembly include:

- Depletion of the low work function material in the cathode insert.
- Failure of the cathode heater due to thermal cycling or erosion.
- Erosion of the cathode orifice plate.
- Erosion of the keeper orifice plate.

The processes which lead to the degradation of cathode inserts are still not understood well enough to allow for a reliable predictive capability regarding their lifetime. Currently, ways to circumvent this problem, such as the development of reservoir cathodes and investigations on the relationship between insert temperature and lifetime are being pursued. A high level of cathode heater reliability has been demonstrated in life tests of hollow cathodes. An engineering model of the space station plasma contactor underwent 3598 successful ignitions during its 28000 hour life.<sup>2</sup> If the heater is subjected to erosion processes, however, a short to the cathode may ensue, resulting in cathode heater failure. Erosion of the cathode orifice plate is also a significant

wear process because the performance of hollow cathodes is sensitive to the geometry of the orifice. If the orifice widens due to erosion, operation of the cathode at the desired electron emission currents and flow rates will eventually become impossible. During a 2000 hour test of an engineering model thruster (EMT), significant erosion of the hollow cathode was observed. An engineering solution to this problem was to include an enclosed keeper electrode into the cathode design. While this was found to nearly eliminate cathode orifice plate erosion, significant wear of the keeper can leave the hollow cathode vulnerable to bombardment by high energy ions, eventually leading to failure of the cathode orifice plate and heater.

From the failure modes mentioned above, it is clear that a better understanding of cathode erosion processes can significantly enhance the capability to predict cathode service life. Furthermore, if keeper wear can be reduced or eliminated, then the lifetime of the cathodes will be improved, since the presence of the keeper serves to mitigate wear processes (b) and (c).

#### Summary of LDT and ELT Erosion Data

In this investigation, a diagnostic technique known as Surface Layer Activation (SLA) was used to measure the erosion of the discharge cathode keeper in an NSTAR configuration ion thruster. Recent long duration wear tests revealed that this component was especially susceptible to rapid wear. During the 8200 hour LDT test of an NSTAR engineering model thruster (EMT2), approximately 30% of the orifice plate of the keeper was worn away, and significant chamfering was found near the orifice during post test analysis.<sup>3</sup> Figure 1 displays this erosion profile, along with the original geometry of the orifice plate. The entire test was conducted at the TH 15 (2.3 kW) set point in the NSTAR throttle table, revealing a maximum erosion rate of approximately 0.064  $\mu\text{m/hr}$ . Similar erosion profiles have been reproduced in a number of other tests conducted under the same conditions. During a 1000 hour test conducted just prior to the LDT, profilometry of the keeper revealed a similar wear pattern with a maximum erosion rate of approximately 0.070  $\mu\text{m/hr}$ .<sup>4</sup> In addition, laser induced fluorescence (LIF) measurements of the highest Mo densities just downstream of the keeper correlate well with the regions of maximum erosion on the keeper surface.<sup>5</sup>

Because the previous life tests were conducted at the maximum throttle level, which was assumed to be the most stressful operating condition for the thruster, comparable wear rates were expected for the ELT, which was to test the flight spare engine (FT2) from the Deep Space 1 (DS1) spacecraft. The ELT vacuum chamber at JPL was equipped with a diagnostics platform which included a camera capable of photographing the keeper through the grids of the

thruster. The camera was of sufficiently high resolution to allow for reasonably accurate measurements of the keeper orifice area as a function of time. Camera images were taken approximately every 3000 hours to characterize the surface evolution of the different thruster components.

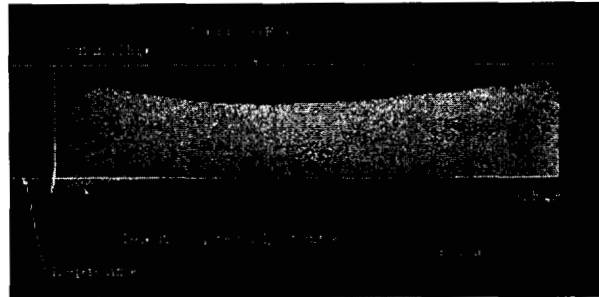


**Figure 1:** Cathode keeper erosion profile from the 8200 hour LDT<sup>3</sup>

Figure 2 displays the surface of the cathode keeper at different stages during the ELT. The photos suggest a much higher than anticipated wear rate of in the ELT based on previous experience with the LDT and the 1000 test. The reasons for this increase are not yet well understood, although some insight may be gained by correlating the photographs with changes in thruster operating conditions. At 4835 hours, the throttle level of the engine was changed from TH 15 to TH 8. After approximately 5935 hours of operation, the keeper shorted to cathode. This condition persisted until approximately 7604 hours, and intermittent shorting continued for approximately 1300 hours afterwards. Photographs of the keeper taken after 4693 and 6408 hours indicate a significant change in the erosion pattern. The photograph at 4835 hours suggests an erosion profile similar to that seen after the 8200 hour test. The photograph taken after 6408 hours of operation displays substantial chamfering of the orifice plate. Rapid widening of the keeper orifice occurred afterwards, and continued even after the thruster was throttled up to TH 15.<sup>4,6</sup>

#### Drawbacks of Long Duration Tests

While long duration tests are valuable for demonstrating thruster lifetimes for future spaceflight applications, the keeper erosion problem highlights some of the drawbacks associated such tests for obtaining erosion data. The LDT and ELT combined represent nearly 6 years of testing, and yet only limited information regarding the factors which affect the keeper erosion has been acquired. Between the two tests, Figure 1 is the only source of an erosion profile for a single operating point. An estimate of the magnitude of the erosion rates may be inferred from the ELT photographs, but a lack of data concerning the

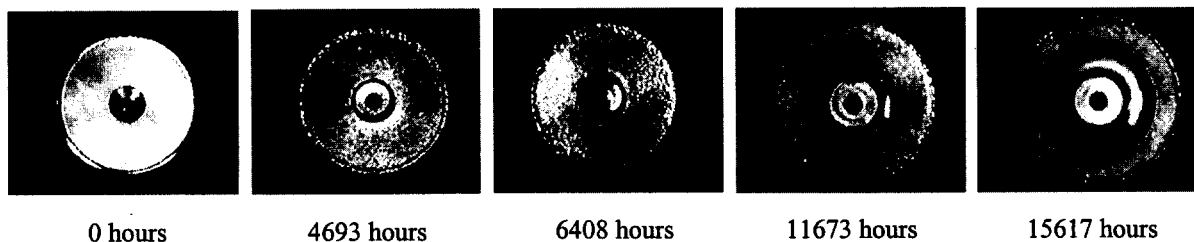


Figure 2: Evolution of the cathode keeper surface during the ELT

eroded depths causes these photos to be of limited value.

Extensive research over the past 45 years has been devoted to evaluating ion thruster service lifetimes. However, to date, long duration wear testing is considered to be the most reliable source of erosion data due to limitations of wear diagnostics. The wide range of throttle levels and lengthy lifetime requirements on modern thruster designs have rendered the reliance on life testing alone impractical, both in terms of time and from a cost standpoint.<sup>1</sup> This necessitates the development of better diagnostic techniques which are capable of accurately measuring the very small wear rates which occur in this type of system in short periods of time.

A further advantage of using erosion diagnostics is the insight which they provide into underlying physics of the ion thruster. Erosion rates at a variety of operating conditions can be used in conjunction with discharge chamber models and sputtering data to achieve a better predictive capability for the effect of a change in operating point will have on the erosion rate.

#### Recent Erosion Diagnostics

Several methods of erosion measurement have been in common use, each with different advantages and drawbacks in terms of spatial resolution, sensitivity, or required testing time. A prominent technique in current use is Laser Induced Fluorescence (LIF). A more detailed discussion of this method may be found in References 5 and 7. The general methodology involves using a precisely tuned laser to excite the target species under investigation. Using this method, sputtered products near the surfaces under investigation can be interrogated, assuming the density of the species in this region is sufficiently high.<sup>2</sup> An alternate method of method of calculating erosion rates via LIF is measuring the velocities of the ion species near a given surface, calculating the ion energies and densities, and extrapolating the erosion rates from this information and existing sputter yield data.<sup>7</sup> The method has the advantage of being non-invasive, and *in-situ*, allowing for a large database of erosion rates to be accumulated in a short period of time over a variety of operating conditions.

As useful as LIF is as a plasma diagnostic technique, several formidable technical challenges inhibit its accuracy as an erosion measurement tool. For example, interrogation of the sputtered products becomes difficult if the densities of these species are low. In addition, to determine the density of sputtered particles, the ratio of the excited state and ground state populations must be calculated. The ratio is a function of electron temperature, which cannot be measured *in-situ* by LIF.<sup>5</sup> Furthermore, if erosion rates are based on ion energies and densities near a surface, reliable sputter yield data at low energies is required. Although recent measurements into this area have greatly improved, the uncertainty in the measurement is sufficiently high to prevent their use as a lifetime prediction tool. Another disadvantage of LIF is the need to have optical access to the desired thruster components. This can be especially problematic for interrogating the sputtered products of the screen grid and discharge cathode. Williams was able to solve this problem for the discharge cathode erosion by adding quartz windows to the side of the thruster and mounting the engine on a two axis positioning stage.<sup>5</sup> In the end, LIF lacks the accuracy required for ion thruster life time assessment.

Profilometry has also seen use in erosion studies, although in many cases the texturing of the sputtered surface makes it difficult to accurately assess the eroded depth. Furthermore, a smooth reference surface is required for comparison, making it necessary to apply masking techniques to the region in question. Often, to obtain detectable eroded depths, lengthy testing time is required. One may substitute materials with higher sputter yields in order conduct accelerated erosion tests. However, the sputter yields of most materials at low energies are not yet well known, making it difficult to correlate erosion data from components fabricated from different materials.

Optical spectroscopy is another method which may be applied to interrogate the sputtered products. In this case, the optical line emission from the sputtered material is detected. The method suffers from many of the same pitfalls as LIF. Optical access to the thruster components is a necessity for these types of measurements. Furthermore, the method can only

provide relative erosion measurements directly. A calculation of excitation rate coefficients is required for the transition being monitored in order to obtain absolute wear rates. Detection of the sputtered products may also be difficult if particle densities are low. As was the case with LIF, electron temperature and number density are required for the interpretation of results, and are generally not well known in the cathode region of the thruster.

### SURFACE LAYER ACTIVATION

Surface Layer Activation circumvents many of the shortcomings of the current methods of measuring erosion. The general technique involves bombarding the material under consideration with a high energy ion beam produced by a particle accelerator or cyclotron. The ions colliding with the surface have a known probability of causing a nuclear reaction which transmutes some of the target atoms to a radioactive isotope. A schematic of this process is shown in Figure 3. Knowledge of the beam energy, angle of incidence, and reaction cross-sections allows the activity per unit depth to be calculated. The activity level of the tracer material may be recorded before a test via a gamma spectroscopy system. After the test is conducted, another spectrum is recorded, and a scaling parameter between the two spectra is determined and correlated with a mass loss rate. Although not as precise as time integrated measurements, SLA may also be applied *in-situ*, by placing the detector near the eroded surface, and monitoring the wear rate in real time. Although the process by which this may be accomplished is well developed, it was not undertaken in this investigation.

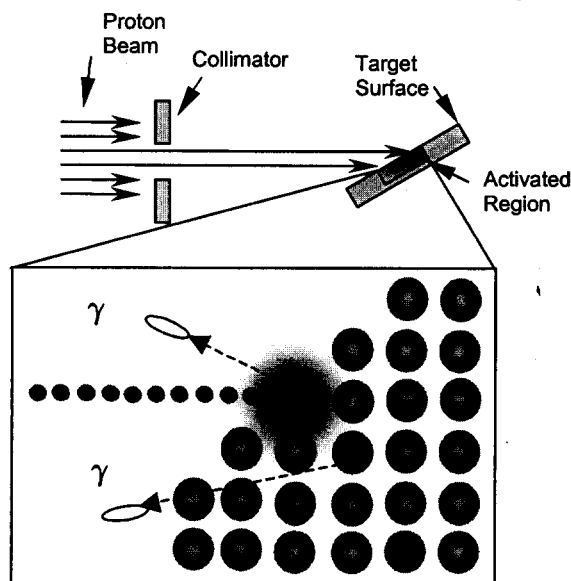


Figure 3: Schematic of the activation process

A major advantage of SLA over other erosion diagnostics is its high sensitivity. Although the *in-situ* measurements were not attempted in this study, reasonable accuracy may be achieved for typical keeper erosion rates after only 40 hours of operation. In addition, since only the material in the activated region is monitored, localized measurements are possible. In general, the width of the activated region is limited only by the beam diameter, which can easily be focused to a spot size of 1mm. Perhaps the best attribute of SLA is the fact that the decrease in activity represents a direct measure of the mass loss. The relationship between the measured signal and the erosion rates is governed by a single depth calibration curve which is known to a high level of accuracy. There is no need to infer erosion rates from the densities or emission spectra of sputtered particles, as is the case with other techniques.

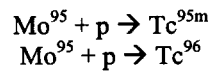
SLA has been used frequently in the automotive industry as a method of measuring wear rates of piston rings in internal combustion engines.<sup>8</sup> In this case, a  $Fe^{56} \rightarrow Co^{56}$  reaction is utilized, and the wear rate is measured in real time by monitoring the radioactivity of the engine oil. It has also been applied to measuring the wear of railway rails and cutting tools, the effectiveness of different lubricants, and in corrosion studies.<sup>9</sup> In materials which can not be directly activated, such as plastics and carbon composites, recoil implantation may be used. In this case, a thin foil is placed in front of the target surface. When the foil is bombarded with an ion beam, some of the atoms in the foil become activated and gain sufficient kinetic energy to leave the foil and imbed in the target surface. The activated depth then depends heavily on the atomic mass of the implanted radioisotope. Typically  $Be^7$  recoil implantation yields activated depths of several microns.<sup>9,10</sup> In electric propulsion applications, SLA has been applied at Princeton University in MPD thruster cathode erosion studies.<sup>10,11</sup>

### Activation Parameters

The activation parameters depend on the target material, the desired reaction products, and the required sensitivity. There are a variety of different activations of metals which are applicable to ion thrusters. Recent advances in SLA have also allowed for activation of carbon components by nuclear implantation. Typically, materials with half lives of several months are ideal for surface layer activation applications, since the decay rate is sufficiently fast to minimize facility contamination hazards, while allowing for a reasonably long testing window. In addition, it is desirable to have only a single reaction product since multiple overlapping photo-peaks require higher resolution equipment, and more complex data analysis procedures. To increase the sensitivity, the proton beam may be

angled with the target surface, thereby compressing the activated region into a thinner layer. This has the effect of increasing the amount of activity per unit depth, allowing for better resolution.

The downstream surfaces of the cathode keepers used in this investigation were identical to those used in the flight thrusters. Details regarding the specific dimensions of these components may be found in Reference [3]. To eliminate any differences in the activation profiles due to surface roughness, the downstream surface of each keeper was polished to a 1 micron finish. The keepers were activated by bombarding the molybdenum orifice plate with a 10.4 MeV proton beam. This resulted in two nuclear reactions which transmuted a small percentage of the  $\text{Mo}^{95}$  to the gamma-emitting technetium isotopes,  $\text{Tc}^{95m}$  and  $\text{Tc}^{96}$ :



The reaction yield for  $\text{Tc}^{96}$  is actually 60 times higher than that of  $\text{Tc}^{95m}$ .<sup>9</sup> However, because its half life is so short, its activity drops to negligible levels after approximately 2 months, allowing the spectrum to be analyzed as though it was produced by one isotope only. High resolution Ge(Li) detector scans confirmed that the  $\text{Tc}^{96}$  contributed only minimally to the total activity measured.

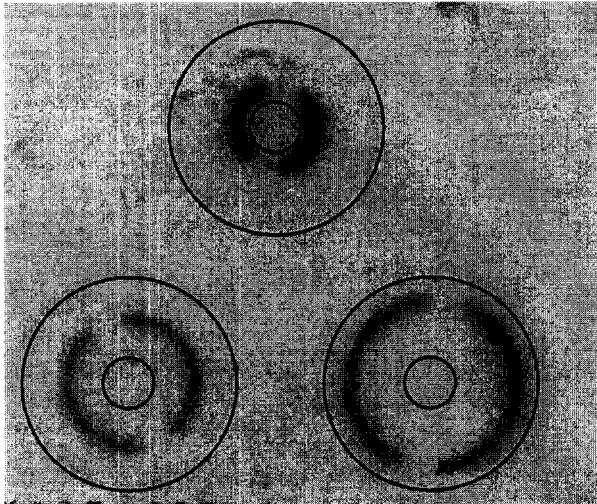


**Figure 4:** Photograph of activated cathode keepers on gamma-sensitive photographic paper (courtesy Kenneth Oxorn). The black outlines indicate the keeper orifice geometry.

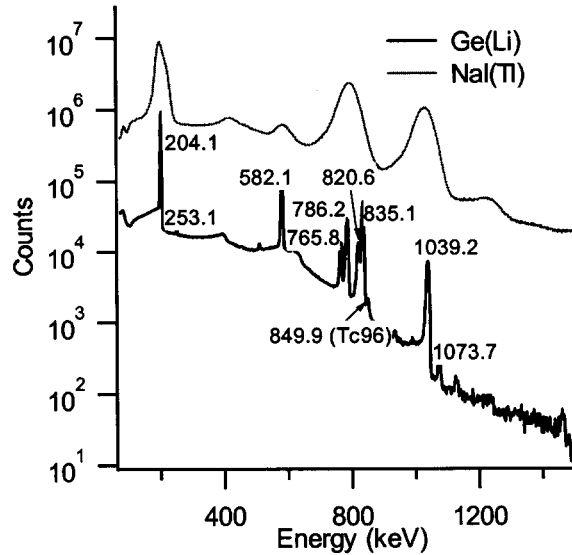


**Figure 5:**  $\text{Tc}^{95m}$  spectra scans from Ge(Li) and NaI(Tl) detectors

Three keepers were activated, each at a different radial location based on the erosion profile which resulted from the 8200 hour test. The activated sites were circular bands concentric with the orifice, each 1 mm thick. A photograph of the activated regions of the keepers using gamma sensitive paper is shown in Figure 4. Note that the gaps in the activated areas are due to the masking technique used during the activation process. The total activity of each band was 2  $\mu\text{Ci}$ , 50% of which was within 30 microns of the surface. To increase the sensitivity of the measurement, the proton beam was angled to 60 degrees with respect to the orifice plate surface. This has the effect of compressing more of the activity in a smaller region near the surface.

#### Calculation of the Depth Calibration Curve

The erosion rates obtained in this study are calculated from the depth calibration curve, which provides the amount of activity remaining in the sample after some level of material loss. The depth calibration used here is derived from both experimental measurements and calculations based on reaction cross section data. The experimental method involves activating a stack of foils of uniform thickness (on the order of several microns.) The activity in each foil may then be measured in relative amounts by gamma spectroscopy. The calculated profile was produced with a software package known as TLAPrf<sup>12</sup> was used. The program utilizes existing foil stack data at known beam energies for 63 different reactions. Empirical relationships and stopping power data from Ziegler's reference volumes [14] are used to extrapolate to intermediate activation energies.

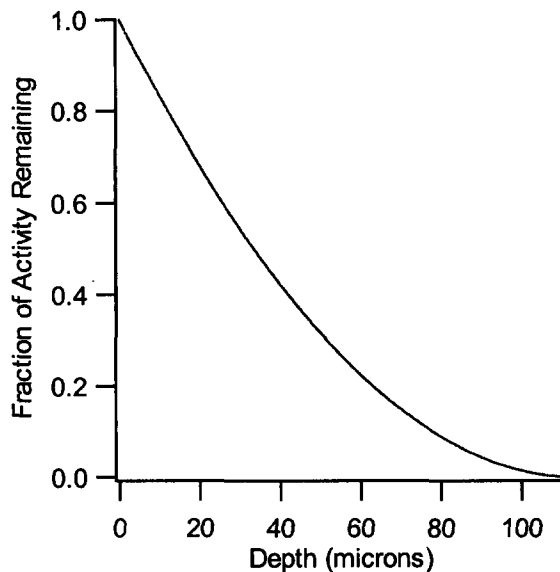


Figure 5: Activity vs. Depth Profile

#### Activity Measurement

The activity of the samples was measured via a gamma spectroscopy system. The detector itself was a NaI(Tl) scintillation detector with a 3 in. by 3 in. cylindrical crystal. The detector crystal emits a number of photons proportional to the energy of the incident gamma that it absorbs. The base of the crystal is attached to a photomultiplier tube (PMT) which generates a voltage signal based on the number of photons emitted by the crystal. The voltage signal is processed by a multi-channel analyzer.

To obtain high resolution scans, a Ge(Li) semiconductor detector available at Caltech was used. The higher resolution was necessary to detect impurities in the activated samples, since the photopeaks from the contaminant isotopes were rather close to those of Tc<sup>95m</sup>. Only one line from Tc<sup>96</sup> could be discerned, at 849.9 keV.

A comparison of the spectra obtained with each type of detector is shown in Figure 4.

Tc <sup>95m</sup>	
Photopeaks (keV)	204.1, 582.1, 1039.2
Half Life	58.72±0.15 days
Tc <sup>96</sup>	
Photopeaks (keV)	778.2, 812.5, 849.9
Half Life	4.28±0.07 days

Table 1: Properties of activated products over the range of interest of this experiment

Although the Ge(Li) detectors offer much better energy resolution, NaI(Tl) detectors were favored in this study. Because the spectrum is essentially comprised of only one isotope, and all of the

photopeaks decay at the same rate, there was no significant penalty for using these types of detectors. Furthermore, the counting efficiency of the NaI(Tl) detectors is superior to the semiconductor detectors. Hence, shorter counting times are required, enabling a faster turnaround time between tests.

#### Data Analysis

The method of resolving the scaling parameter between the gamma spectra is an iterative least squares scheme. This method has been successfully employed in the past at Oak Ridge National Laboratories to determine the concentrations of radioactive contaminants in chemical solutions.<sup>15</sup> The method was later enhanced to allow for the measurement of MPD thruster wear rates.<sup>12</sup>

The sample count rate in a particular channel  $i$  is given by:

$$y_i = \frac{z_i^s}{\tau_s} - \frac{z_i^b}{\tau_b}$$

The sample spectrum may be the composite of several reference spectra. The count rate in a particular channel  $i$  produced by an isotope  $j$  is given by:

$$a_{ij} = \frac{z_{ij}^r}{\tau_{ij}^r} - \frac{z_{ij}^b}{\tau_{ij}^b}$$

The relationship between the two spectra is:

$$y_i = a_{ij}m_j + \varepsilon_i$$

The objective of the weighted least squares method is to find a solution  $\hat{m}$  which minimizes the error term  $\varepsilon_i$  according to some weight factor matrix  $W_{ij}$ . The diagonal elements of  $W$  are generally the inverse of the count rates in each of the channels, in order to mitigate the effect of peak broadening in the experimental data. As a result, the best fit provided by the least squares method is given by:

$$\hat{m}_j = (W_{ii}a_{ij}a_{ik})^{-1}(W_{ii}a_{ij}a_{ik})$$

Large errors may occur if there is significant gain and threshold drift in the instrument electronics. The least squares methodology is ideally suited to correcting for such errors. Details of the implementation of these methods may be found in either of References [12] or [15].

#### Error Analysis

The greatest advantage in using SLA to measure extremely low wear rates is the high level of accuracy which is attainable. To ensure this level of accuracy is achieved, a careful examination of sources of error is necessary.

Error in the scaling parameter between the sample and reference spectrum arises from statistical fluctuations in the count rate of each channel. This uncertainty is given by:<sup>13</sup>

$$\hat{\sigma}^2(m_j) = \frac{1}{n-h} \left( W_{ii} a_{ij} a_{ij} \right)^{-1} W_{ii} \left( y_i - a_{ij} m_j \right)^2$$

Note that for a given channel, the statistical fluctuation is:

$$\sigma^2(y_i) = \frac{y_i^s + y_i^b}{\tau^s} + \frac{y_i^b}{\tau^b}$$

From this relationship it is clear that the two steps which may be taken to effectively reduce the variance in count rates include reducing the background count rate by surrounding the detection system with lead shielding, and increasing the collection live times. In this study, collection times in excess of  $10^4$  seconds were used, making statistical noise an insignificant source of error in the measurements.

The photomultiplier tube of the detection system also introduces a potentially significant error source. The PMT heats up during operation causing amplifier gain and threshold shifting. To eliminate this effect, a software gain stabilization is implemented as the spectrum is being collected. The gain is actively controlled so as to maintain a single photopeak in a specified energy window. This is sufficient to nearly eliminate threshold shifting, and to hold the gain shifting to within 3%. A secondary software correction is used after the spectra are collected to completely eliminate the gain shifting. As a result, this type of error is not expected to contribute significantly to the measurement error.

Another factor affecting the measurement precision is the uncertainty in the half life of  $Tc^{95m}$ . The best estimate to date for this value is  $61 \pm 2$  days, derived from a 1959 paper by Unik and Rasmussen. This value was arrived at by a technique known as "peak stripping", which is less accurate than the least squares fitting scheme employed in this study. Analysis of a pure  $Tc^{95m}$  sample revealed a half life of  $58.72 \pm 0.15$  days. The improved estimate is due primarily to enhancements in the analysis method (iterative least squares), and the fact that technetium can be more readily produced in a purer form today than when the previous study was undertaken. The accuracy of this measurement also demonstrates the repeatability and precision of this measurement technique over a long period of time.

In addition, the trace amounts of  $Tc^{96}$  remaining in the activated samples during the early portion of the testing also affected the count rates. Typically, the  $Tc^{96}$  contribution to the spectrum was less than 0.33% of the total number of counts. Furthermore, the short half life of this isotope (4.2 days) made it significant only in the first two tests conducted. The error due to the decay of these contaminants is a slight over prediction of the wear rate.

The depth calibration curve was expected to be the largest source of error in the SLA measurements.

The error arises from how well the fitting functions match the foil stack data. In general, agreement is best in the shallow regions of the curve (which for this experiment is between 0 and 15  $\mu m$ ). The curve is nearly linear over this depth range. Calculations of linear fits for foil stack data at 7, 10, 11, and 22 MeV indicated a worst case error in slope of  $\pm 10\%$ .

There are also uncertainties introduced by the wear process itself. If the eroded depth is uneven across the activated region, the perceived depth may be skewed depending on the shape of the depth calibration curve in this region, and the degree to which the erosion is non-uniform. However, in since the experiments in this study used only the portion of the depth calibration curve which was nearly linear, any such effects would be averaged out.

The combination of the above parameters provides a fairly complete treatment of the errors associated with the measurement itself. The error analysis performed above suggests an uncertainty of approximately .3 microns in the measured values. The remaining errors in these experiments therefore are associated with the performance of the thruster itself, which are more difficult to quantify. Because wear rates are being measured over a rather short period of time, it is essential that the thruster operating parameters be stable for the duration of each test, and that the thruster performance be reproducible with each iteration. Generally the performance of the thruster was fairly stable during a typical test. After start-up, the engine parameters generally stabilized after approximately 20 to 30 minutes of operation. The thruster appeared to perform similarly between subsequent tests, although over time the performance of the engine was noted to degrade with repeated exposures to atmosphere. Although the cathodes were reconditioned at the beginning of each test, it is suspected that the repeated exposure to the water vapor and oxygen in the air had an unfavorable effect on the cathode inserts, causing a small increase in discharge voltage and neutralizer keeper voltage with time. Because it is not yet known how these parameters affect discharge keeper erosion, the error bars for the measurements presented in this study indicate only the measurement error. The uncertainty in the engine operating parameters is included with the erosion data for reference.

## RESULTS

### Erosion Characterization Experiments

A major challenge for this study was to construct a laboratory thruster which faithfully reproduced the characteristics of the DS1 ion engine since contamination concerns precluded using any of the EMT's. As a result, a laboratory model of the NSTAR thruster (known as the "NKO thruster") was developed

for use in this study. The discharge chamber is of aluminum construction, with the magnets themselves and their placement identical to those used on the flight engines. Detailed magnetic field maps of the cathode region of NKO and EMT2 indicated that the field strength was accurately replicated. In addition, the orifice plates of the laboratory model cathode and keeper were also identical to those of FT1 and EMT2. Detailed descriptions of the geometries of these components may be found in [3]. The thruster was outfitted with a molybdenum grid set from a J-Series thruster. The grids were fabricated with the same hole geometry as the later NSTAR series thrusters.

All testing was conducted in JPL's 2.5 x 5.5 m Thruster Performance and Endurance Test Facility. The chamber is equipped with an ExB probe, and two Faraday Probes. The power supply system was comprised of components similar to those used on the recently completed ELT. A data acquisition system also similar to that in use on the ELT allowed for continuous monitoring of the thruster parameters to enable unattended operation.

A preliminary test was conducted to verify that the thruster performed similarly to the DS1 ion thruster over the entire NSTAR throttle range. In general, the agreement with the throttle table values was excellent, as demonstrated in Table 3. Furthermore, the ExB probe data and keeper ion also matched closely with those measured during an earlier series of tests with EMT4.



**Figure 6:** The NKO thruster in the 2.5 x 5.5 m vacuum test facility at JPL

A total of 9 tests were conducted, each between 40 and 70 hours in duration. The objectives of the erosion tests were to validate the SLA method as a viable wear diagnostic for ion thrusters, to determine the dependence of keeper erosion on thruster power levels, and to investigate the variation of wear rate due

to changes in the keeper potential. Two operating points (TH 8 and TH 15) were considered, because of the large amount of ELT available for these two points.

In addition to the nominal operating conditions, several tests were conducted with the cathode keeper biased at different potentials. Two methods were used to accomplish this task. First, an adjustable resistor was wired in parallel with the 1 k $\Omega$  resistor which typically couples with anode to the keeper. In subsequent cases, the keeper was biased positive with a 0-30V power supply.

### Regions of Deposition

Although not the primary goal of this study, it is also of interest to determine the areas where the sputtered material from the keepers is most heavily deposited. Measurement of sputter-deposited material using radioactive tracer methods has been attempted in the past as a technique to characterize the sputter yields of Co and Cr at low energies. The disadvantage of this method is that in order to obtain an absolute measurement of the amount of material that has been deposited, relatively high activities are required so that the counting statistics are sufficiently good for a reliable comparison to a known radioactive sample source. In general this usually requires activities in the mCi range, which is an order of magnitude higher than the radioactivity level used in these experiments.

Because of these difficulties, absolute measurements of the quantity of material deposits were not attempted. However, the gamma signal from the deposits was sufficiently strong to allow for the calculation of relative quantities on the inside of the thruster. To accomplish this, nine stainless steel witness plates were attached to the thruster interior, including one on the cathode flange, 4 on the conical section of the discharge chamber, and 4 on the cylindrical portion. The locations of these plates are displayed in Figure 8. The thruster was operated at TH 8 with the keeper activated along the inner-most in place. The plates were removed after the test, and their gamma spectrum was obtained.

An alternate analysis method was used to assess the relative activities of the witness plates. A peak finding algorithm calculated the location of the 204 keV and 1040 keV gamma peaks in the Tc<sup>95m</sup> spectrum. Using this as the range of interest, the total number of counts between these two peaks was calculated. The statistical uncertainty in the number of counts in this range is given by:

$$\sum_i \sigma^2(y_i) = \sum_i \frac{y_i^a + y_i^b}{\tau^a} + \frac{y_i^b}{\tau^b}$$

## RESULTS

### NKO Thruster Performance Data:

TH Level	$\dot{m}_{cath}$ (sccm)	$\dot{m}_{neut}$ (sccm)	$\dot{m}_{main}$ (sccm)	$V_B$ (V)	$J_B$ (A)	$V_A$ (V)	$J_{NK}$ (A)
8	2.47	2.40	14.41	1100	1.10	-180	1.5
15	3.70	3.60	23.42	1100	1.76	-250	1.5

Table 2: Thruster set points for TH 8 and TH 15

TH Level	$J_D$ (A)	$V_D$ (V)	$J_A$ (A)	$V_{NK}$ (V)	$P_{TOR}$ (W)	$T$ (mN)	$I_{sp}$ (sec)	$\eta_{TOR}$
0	4.54	24.91	1.94	17.39	480.97	21.01	1986.33	0.4257
3	5.61	26.42	2.01	16.67	853.35	32.38	2836.91	0.5280
6	7.43	24.64	3.70	15.38	1217.24	48.30	3067.00	0.5970
8	8.56	24.19	5.04	15.41	1443.55	58.49	3116.12	0.6193
12	10.97	24.33	8.43	14.60	1935.37	79.23	3185.76	0.6397
15	14.16	23.00	11.30	13.99	2293.62	93.66	3132.88	0.6275

Table 3: NKO performance data over the entire NSTAR throttle range

TH Level	Keeper Ion Saturation Current	J++/J+
8	127 mA	0.273
15	191 mA	0.303

Table 4: NKO keeper ion current and double ion current along thruster centerline

### Erosion Data:

$r/r_0$	Test Duration (hrs)	8200 Hour Erosion Rate ( $\mu\text{m/hr}$ )	Measured Erosion Rate ( $\mu\text{m/hr}$ )	Mass Loss Rate ( $\mu\text{g/hr-mm}^2$ )	$V_D$ (V)	$V_{CK}$ (V)
0.341	70.9	0.0387	0.0546 <sup>+0.0014</sup> -0.0019	0.562 <sup>+0.015</sup> -0.020	23.86±0.24	3.39±0.10
0.540	80.4	0.0629	0.0853 <sup>+0.0020</sup> -0.0040	0.877 <sup>+0.021</sup> -0.041	24.07±0.21	3.32±0.17
0.735	74.8	0.0508	0.0589 <sup>+0.0014</sup> -0.0016	0.605 <sup>+0.015</sup> -0.016	23.92±0.15	3.51±0.10

Table 5: TH 15 erosion rate test results

$r/r_0$	Test Duration (hrs)	Measured Erosion Rate ( $\mu\text{m/hr}$ )	Mass Loss Rate ( $\mu\text{g/hr-mm}^2$ )	$V_D$ (V)	$V_{CK}$ (V)
0.341	39.7	0.0401± 0.0032	0.412± 0.033	24.72±0.19	2.48±0.06
0.540	44.5	0.0291± 0.0041	0.298± 0.042	24.69±0.22	2.57±0.10

Table 6: TH 8 erosion rate test results

$r/r_0$	Test Duration (hrs)	Measured Erosion Rate ( $\mu\text{m/hr}$ )	Mass Loss Rate ( $\mu\text{g/hr-mm}^2$ )	$V_D$ (V)	$V_{CK}$ (V)
0.341	76.0	0.0311± 0.0030	0.320± 0.032	25.42±0.22	7.88±0.14
0.341	86.5	0.0349± 0.0033	0.359± 0.034	Fill in	Fill in
0.341	39.7	0.0401± 0.0032	0.412± 0.033	24.72±0.19	2.48±0.06
0.341	44.7	0.0538± 0.0041	0.553± 0.042	24.76±0.24	0 (Shorted)

Table 7: TH 8 erosion rates with different keeper potentials

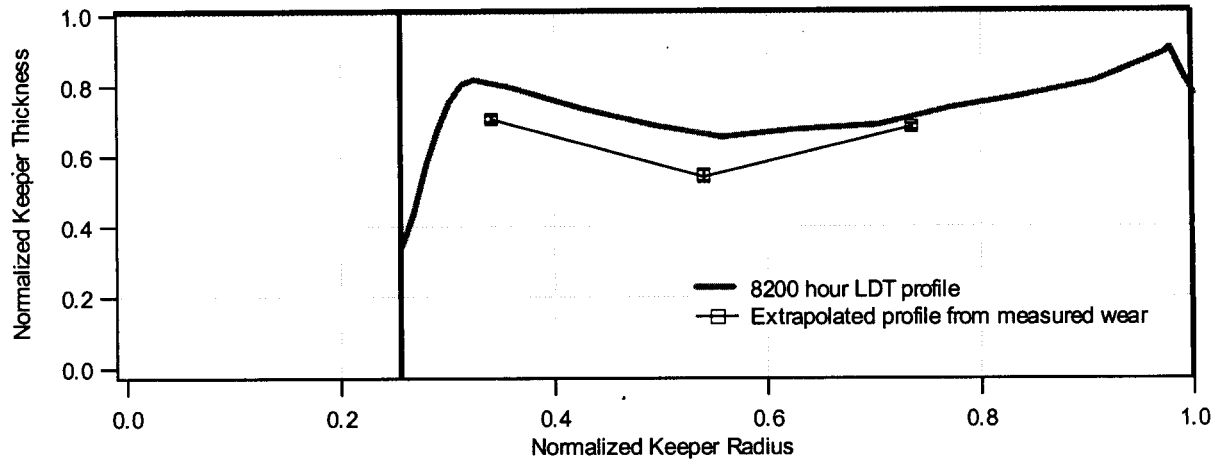


Figure 7: Extrapolated erosion profile after 8200 hours of operation at TH 15. The LDT profile is included for comparison.

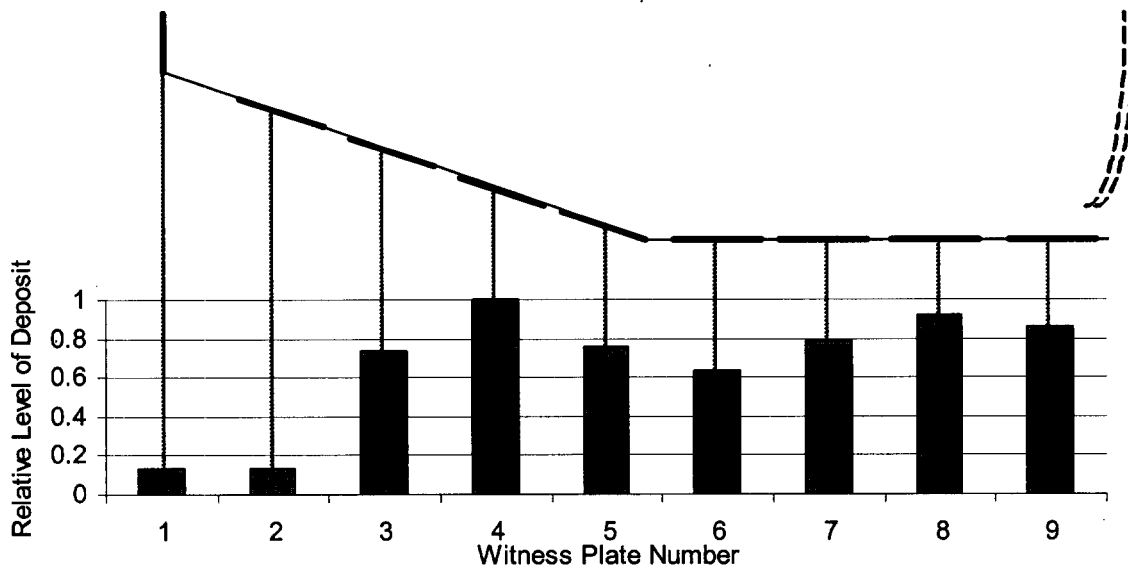


Figure 8: Relative levels of deposition inside the discharge chamber

## DISCUSSION

The measured erosion rates at TH 15 agreed closely with the 8200 test profile. In each case, the erosion rate is 15% to 25% higher than the LDT data. It is likely that this increase in erosion was due to the keeper electrode floating approximately 0.5V lower than average value of EMT2. After the tests were completed, noticeable texturing of the keeper surfaces was observed, as shown in Figures 9 and 10.



Figure 9: Pre-Test Keeper Photo

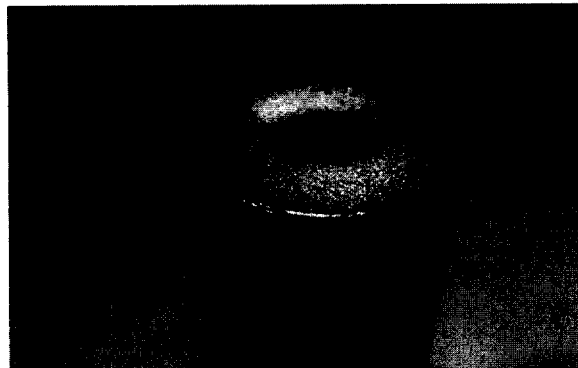


Figure 10: Post-Test Keeper Photo after 70 hours of operation at TH 15

Recall that it was suspected from the ELT that significant erosion of the cathode keeper occurred once the operating point was changed to TH 8. Erosion data with the NKO thruster at this operating point displays two important attributes. First, the wear rates appear to be less overall at this lower throttle level than at TH 15. In addition, a different wear profile is shown with the most severe wear near the orifice.

The erosion data from the tests at TH 8 are shown in Table 6 and in Figure 11. The erosion rates mentioned above would not be sufficient to cause the rapid wear observed in the ELT. However, the increased erosion rates near the keeper orifice may provide an explanation for the chamfering observed in the ELT photographs. Recall that after the switch to the TH 8 throttle setting the keeper shorted to cathode. It is

likely that the decrease in keeper potential caused the increased wear rates observed in the ELT.

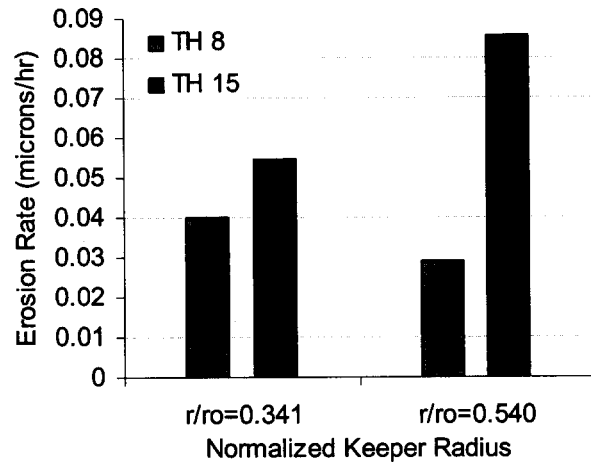


Figure 11: Erosion rate comparison for TH 8 and TH 15

### Variation of Erosion Rate with Keeper Potential

Based on the data obtained from the previous battery of tests, it was suspected that the keeper voltage substantially influenced the erosion rate. If the conservation of energy at a surface immersed in a plasma is considered, one can calculate the ion energies of a given species at the surface:

$$E_w = E_o + q(V_D - V_K)$$

Hence, increasing the voltage difference between the discharge chamber and the cathode keeper would result in higher ion energies at the keeper surface. It is reasonable to conclude that increasing the keeper voltage may reduce the erosion rate.

To verify this hypothesis, four tests of the inner activated region were conducted, with the keeper biased to different potentials. The purpose of these tests was to compare the nominal operating point with a shorted and biased keeper case. The results from this analysis are displayed in Table 7 and Figure 12. When the keeper is shorted to cathode the erosion rate increases significantly.

Furthermore, increasing the keeper potential has shown to reduce the erosion rate. This was accomplished by decreasing the resistance between keeper and anode, allowing it to float at a high potential. This coupled with using a carbon keeper could serve to eliminate or significantly reduce the erosion of the discharge cathode assembly.

Note that the erosion shorted TH 8 operating condition at  $r/r_o=0.341$  is comparable to the TH 15 nominal case at the same position. Based on the ELT photographs, this suggests that much of the erosion may occur on the side wall of the orifice hole. An activation

on the side wall could easily be achieved and will be attempted in the next batch of keeper erosion tests.

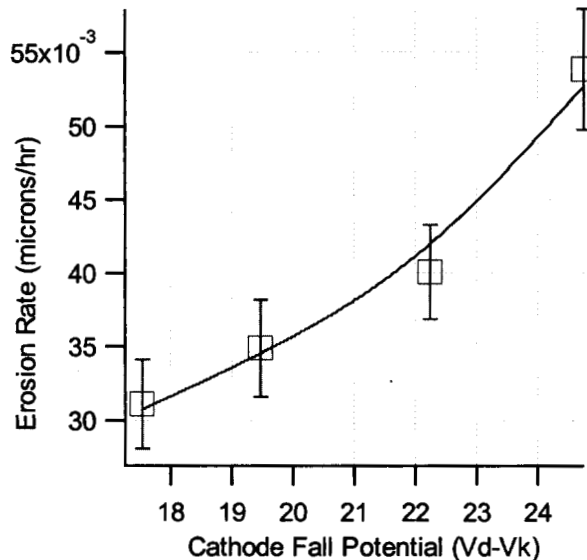


Figure 12: Erosion rates as a function of keeper potential

#### Repeatability

Although it was impractical to perform multiple tests for the same thruster operating conditions, it was desirable to examine the repeatability of results between the beginning of the test cycles to the end. A test of the keeper activated at  $r/r_0=0.735$  for the TH 15 setting was conducted twice. The measured wear rates correspond closely with each other (to within 9%).

#### Future Work

The SLA technique will continue to be applied to a study of keeper erosion. The next batch of tests will include a cathode keeper which has been activated on the side wall of the orifice. This measurement would help to explain whether or not the rapid erosion witnessed at the TH 8 operating condition was primarily due to widening along the orifice wall.

The technique may also be applied to future propulsion projects which will use hollow cathode assemblies, such as NEXT and NEXIS. A keeper erosion study for both of these projects is a feasible option. In addition, a tungsten activation is applicable to cathode orifice erosion. With a high resolution detection system, both measurements could be carried out simultaneously.

Eventually, these erosion measurements could be coupled with other diagnostic techniques to formulate a model of keeper erosion. Ways to measure the ion current to different radii along the keeper surface are being investigated. Knowledge of the ion energies at the keeper surface and accurate

measurements of sputter yields at low energies would also be necessary to model keeper wear.

### CONCLUSIONS

The surface layer activation method was validated in this investigation by reproducing the wear pattern observed in the 8200 hour LDT at TH 15. The TH 8 erosion profile was found to differ significantly from the TH 15 profile. At TH 8, the wear is greatest near the orifice, as compared to the TH 15 condition, where the wear is largest near the middle of the profile. In addition, at the nominal TH 8 case, the erosion rates were significantly less than at TH 15.

Keeper potential appears to have a significant effect on the erosion rate. Four tests conducted at TH 8 indicate that the erosion rate increases significantly when the keeper is shorted to cathode. Furthermore, biasing the keeper to a higher positive voltage can be used as a technique to combat erosion.

Wear tests on a laboratory model thruster produced erosion data for 8 different operating conditions, each after only 40 to 70 hours of operation. Evaluation of this number of conditions using conventional long duration testing would have required thousands of hours of operation. Tests similar to these could be applied to future propulsion projects, such as NEXT and NEXIS to accurately measure the erosion rates of cathode and grid components.

### ACKNOWLEDGEMENTS

The authors gratefully acknowledge Ken Oxorn of ANS Technologies for his valuable assistance in the activation process. They would also like to thank Al Owens at JPL for his skill in fabricating the ~~MC~~ NKO thruster. The research described in this paper was conducted in part at the Jet Propulsion Laboratory, California Institute of Technology, and was sponsored by the National Aeronautics and Space Administration.

### REFERENCES

- [1] Brophy, J.R., Polk, J.E., and Rawlin, V.K. "Ion Engine Service Life Validation by Analysis and Testing". AIAA-96-2715.
- [2] Sarver-Verhey, T. R., and Hamley, J.A. "Discharge Ignition Behavior of the Space Station Plasma Contactor". AIAA-94-3311.
- [3] Polk, J.E., et. al. "An Overview of the Results from an 8200 Hour Wear Test of the NSTAR Ion Thruster". AIAA-99-2446.
- [4] Domonkos, Matthew T., Foster, John E., and Patterson, Michael J. "Investigation of Keeper Erosion in the NSTAR Ion Thruster". IEPC-01-308.
- [5] Williams, G.J., Smith, T.B., and Gallimore, A.D. "30 cm Ion Thruster Discharge Cathode Erosion". IEPC-01-306.

- [6] Anderson, J.R., et. al. "Long Duration Ground Testing of the Deep Space 1 Flight Spare Ion Thruster – the First 15600 Hours". IEPC-01-076.
- [7] Domonkos, M. T., and Williams, G. J. "Status of Real-Time Laser Based Ion Engine Diagnostics at NASA Glenn Research Center". IEPC-01-304
- [8] Kosako, T. and Kazuo, N. "The Thin Layer Activation Technique Applied to the On-Line Iron Wear Measurement of an Engine Cam Nose". *Nuclear Instruments and Methods in Physics Research B*. Vol 56/57, 1991.
- [9] Report, IAEA TECDOC-924, *Thin Layer Activation Method and its Application in Industry*.
- [10] Ditrói, F., and Mahunka, I. "Thin Layer Activation of Non-Metallic Materials by Using Nuclear Implantation". *Nuclear Instruments and Methods in Physics Research B*. Vol. 113, 1996
- [11] Marks, L. M., Clark, K. E., and et. al. "MPD Thruster Erosion Measurement". AIAA-82-1884.
- [12] Polk, J.E. *Mechanisms of Cathode Erosion in Plasma Thrusters*. Ph.D. Thesis, Princeton University, 1995.
- [13] G. Wallace. "Calculation of depth profile for thin layer activation". Client Report, 62891H 11, Prepared for IAEA Contract C3-544, Project RAS/8/078, March 1999, unpublished.
- [14] Ziegler, J.E., Biersack, J.P., and Littmark, U. *The Stopping and Range of Ions in Solids*. Vol. 1, Pergamon Press, 1985.
- [15] Schonfeld, E., Kibbey, A.H., and Davis, Jr., W. "Determination of Nuclide Concentrations in Solutions Containing Low Levels of Radioactivity by Least-Squares Resolution of the Gamma-Ray Spectrum". *Nuclear Instruments and Methods*. Vol. 45, 1966.